

# CRISPR-based editing strategies to rectify *EYA1* complex genomic rearrangement linked to haploinsufficiency

Hwalin Yi,<sup>1,7</sup> Yejin Yun,<sup>2,7</sup> Won Hoon Choi,<sup>2,7</sup> Hye-Yeon Hwang,<sup>1,7</sup> Ju Hyuen Cha,<sup>2</sup> Heeyoung Seok,<sup>3</sup> Jae-Jin Song,<sup>4</sup> Jun Ho Lee,<sup>2</sup> Sang-Yeon Lee,<sup>2,5,6</sup> and Daesik Kim<sup>1</sup>

<sup>1</sup>Department of Precision Medicine, Sungkyunkwan University School of Medicine, Suwon 16419, Republic of Korea; <sup>2</sup>Department of Otorhinolaryngology, Seoul National University College of Medicine, Seoul National University Hospital, Seoul 03080, South Korea; <sup>3</sup>Department of Transdisciplinary Research and Collaboration, Genomics Core Facility, Biomedical Research Institute, Seoul National University Hospital, Seoul 03080, South Korea; <sup>4</sup>Department of Otorhinolaryngology, Seoul National University College of Medicine, Seoul National University Bundang Hospital, Seongnam, South Korea; <sup>5</sup>Department of Genomic Medicine, Seoul National University Hospital, Seoul 03080, Republic of Korea; <sup>6</sup>Sensory Organ Research Institute, Seoul National University Medical Research Center, Seoul 03080, Republic of Korea

**Pathogenic structure variations (SVs) are associated with various types of cancer and rare genetic diseases. Recent studies have used Cas9 nuclease with paired guide RNAs (gRNAs) to generate targeted chromosomal rearrangements, focusing on producing fusion proteins that cause cancer, whereas research on precision genome editing for rectifying SVs is limited. In this study, we identified a novel complex genomic rearrangement (CGR), specifically an *EYA1* inversion with a deletion, implicated in branchio-oto-renal/branchio-oto syndrome. To address this, two CRISPR-based approaches were tested. First, we used Cas9 nuclease and paired gRNAs tailored to the patient's genome. The dual CRISPR-Cas9 system induced efficient correction of paracentric inversion in patient-derived fibroblast, and effectively restored the expression of *EYA1* mRNA and protein, along with its transcriptional activity required to regulate the target gene expression. Additionally, we used CRISPR activation (CRISPRa), which leads to the upregulation of *EYA1* mRNA expression in patient-derived fibroblasts. Moreover, CRISPRa significantly improved *EYA1* protein expression and transcriptional activity essential for target gene expression. This suggests that CRISPRa-based gene therapies could offer substantial translational potential for approximately 70% of disease-causing *EYA1* variants responsible for haploinsufficiency. Our findings demonstrate the potential of CRISPR-guided genome editing for correcting SVs, including those with *EYA1* CGR linked to haploinsufficiency.**

## INTRODUCTION

Pathogenic structure variations (SVs) and genomic rearrangements are observed in various types of cancer and rare genetic diseases.<sup>1</sup> Genomic rearrangements are alterations in the architecture of genomic DNA that can result in complex structures, such as inversions, deletions, duplications, and translocations.<sup>1</sup> These genomic rearrangements can arise from DNA double-strand breaks (DSBs) and

incorrect rejoining of the DNA ends via mechanisms such as non-allelic homologous recombination and non-homologous end-joining.<sup>1</sup> Chromosome microarrays and multiplex ligation-dependent probe amplification (MLPA) have become routine real-world techniques for detecting abnormal copy numbers,<sup>2</sup> but genomic approaches cannot identify balanced SVs, such as inversions and translocations. With the diagnostic and technical availability of whole-genome sequencing (WGS), a range of SVs, including complex genomic rearrangements (CGRs), can be identified at a much higher resolution than previously,<sup>3</sup> which leads to a better understanding of their mechanisms and potential therapeutic targets.

The CRISPR-Cas9 system has been adapted for site-specific genome editing in diverse cell types and model organisms.<sup>4,5</sup> Cas9 nuclease generates a DNA DSB at target sites, which induces the cellular repair process through either homology-directed repair or non-homologous end-joining pathways. The development of advanced CRISPR nuclease using paired guide RNAs (gRNAs) achieves precise targeted gene deletions and replacement in human cells.<sup>6</sup> Furthermore, recent studies have used Cas9 nuclease in combination with paired gRNAs to generate targeted chromosomal rearrangements, focusing on cancer-associated chromosomal rearrangements such as *EML4-ALK*, *NPM-ALK*, *CD74-ROS1*, *KIF5B-RET*, *EWSR1-FLI1*, and *AML1-ETO*.<sup>7-10</sup> Previous studies have primarily focused on generating fusion proteins implicated in cancer, whereas the field of precise genome editing for correcting SVs requires further exploration.

Received 21 December 2023; accepted 21 April 2024;  
<https://doi.org/10.1016/j.omtn.2024.102199>.

<sup>7</sup>These authors contributed equally

**Correspondence:** Sang-Yeon Lee, Department of Otorhinolaryngology, Seoul National University College of Medicine, Seoul National University Hospital, Seoul 03080, South Korea.

**E-mail:** [maru4843@hanmail.net](mailto:maru4843@hanmail.net)

**Correspondence:** Daesik Kim, Department of Precision Medicine, Sungkyunkwan University School of Medicine, Suwon 16419, Republic of Korea.

**E-mail:** [dskim89@skku.edu](mailto:dskim89@skku.edu)



Through WGS, we identified a novel CGR, characterized by an *EYA1* inversion with a deletion, responsible for branchio-oto-renal/branchio-oto (BOR/BO) syndrome. BOR/BO syndrome refers to a dominantly inherited rare disease, characterized by branchial anomalies, hearing loss, and renal anomalies. Despite a high penetrance of hearing impairment, with more than 90% of individuals affected,<sup>11,12</sup> the clinical presentation of BOR/BO syndrome is highly variable.<sup>12,13</sup> *EYA1* is a primary disease-causing gene for BOR/BO syndrome, accounting for 40%–75% of patients.<sup>14,15</sup> *EYA1* binds to promoter sequences and engages with general transcription factors.<sup>16</sup> It primarily forms a bipartite transcription factor (*EYA1*-*SIX1*-DNA complex) that controls critical early inductive signaling events involved in ear and kidney formation.<sup>17</sup> Furthermore, the evolutionarily conserved Pax-Eya-Six regulatory hierarchy<sup>17</sup> and *Eya1*-centered multiprotein networks<sup>16</sup> have been shown to elucidate the development of the inner ear, branchial arch-derived organs, and kidney in a distinct manner. Thus, pathogenic variants of *EYA1* that affect functional domains, such as the *Eya* domain, are likely to have molecular consequences in the context of transcriptional activity, resulting in BOR/BO phenotypes. The CGR results in a loss-of-function allele and thus haploinsufficiency served as the underlying mechanism. To rectify this, we developed two genome editing approaches. The Cas9 nuclease and paired gRNAs precisely induce the paracentric inversion to correct the CGR mutation with relatively high efficiency in patient-derived fibroblasts. This dual CRISPR-Cas9 system successfully restores the expression level of the *EYA1* gene, coupled with the expression of downstream target genes, leading to an improvement in transcriptional activity. In addition, through CRISPR activation (CRISPRa), the expression level of both the *EYA1* gene and its encoded protein were increased similar to wild-type levels in patient-derived fibroblasts and human *EYA1* monoallelic knockout cells that mimic haploinsufficiency. The CRISPRa system significantly improved transcriptional activity essential for target gene expression, suggesting such advancements might be relevant to all disease-causing variants associated with *EYA1* haploinsufficiency.

## RESULTS

### Identification of a novel CGR in the *EYA1* gene

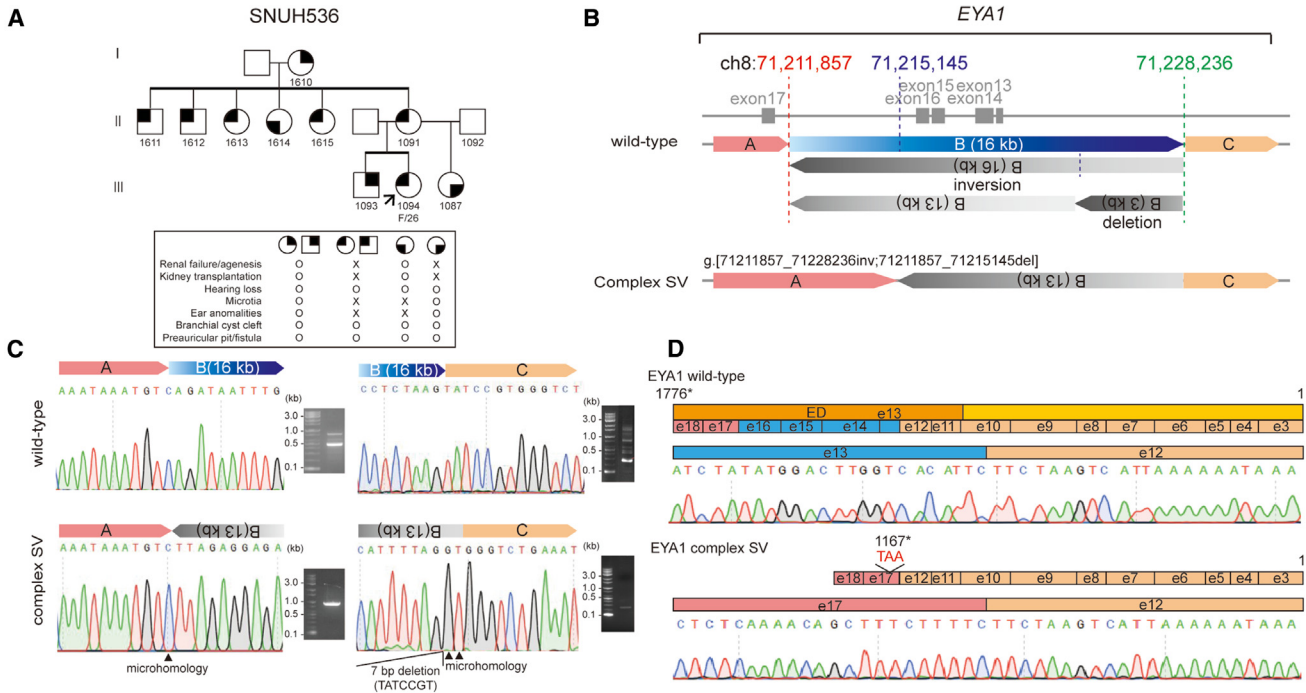
The proband, a 27-year-old (SNUH536-1094), manifested bilateral mixed hearing loss, bilateral preauricular fistulas, and a history of discharge from tiny neck openings on each side. The mother of the proband and affected siblings in SNUH536 family exhibited a range of clinical phenotypes associated with BOR/BO syndrome, demonstrating complete penetrance but variable expressivity of clinical phenotypes (Figure 1A). A bioinformatics approach and filtering strategy of WGS results, aimed at prioritizing candidate causal variants for BOR/BO syndrome, yielded negative results. The sequential MLPA test showed a normal copy number state in *EYA1* gene (Figure S1). A thorough examination of a region on chromosome 8 was conducted by leveraging SV profiles via family-based WGS. This process revealed a novel CGR involving an *EYA1* inversion (g.71211857 to g.71228236; with a 5'-breakpoint in intron 16 of *EYA1* and a 3'-breakpoint in intron 12 of *EYA1*), with a deletion at the end of the segment (g.71211857 to g.71215145; with both the 5'-breakpoint and 3'-break-

point located in intron 16) (Figures 1B and S2). We identified two neo-junctional reads, one with 1 bp of microhomology (A-B, g.71215145) and the other with 2 bp of microhomology (B-C, g.71228236) (Figure S3). To confirm the breakpoint junctions identified by WGS, we designed four pairs of forward and reverse primers (Table S1). Gap-PCR revealed the amplification of a 954-bp PCR product corresponding to the breakpoint within intron 16 (A-B junction) and a 235-bp PCR product corresponding to the breakpoint within intron 12 (B-C junction) (Figure 1C). We also verified the genomic sequence of junctions by Sanger sequencing (Figure 1C). To further identify the *EYA1* mutant allele, cDNA Sanger sequencing of the coding regions of *EYA1* CGR was performed. The gel electrophoresis image displaying the RT-PCR results, including conditions treated with cycloheximide (CHX) to inhibit nonsense-mediated mRNA decay (NMD), and primer sets used for cDNA Sanger sequencing is described in Table S2. The cDNA-level consequences were revealed the removal of the sequence from the inverted exons 13–16 of *EYA1* CGR, leading to a novel NM\_000503.6:r.1141\_1597del variant. This premature stop codon results in a truncated non-functional protein (p.Cys382Lysfs\*7), a region that includes the functional *Eya* domain (Figure 1D), which is predicted to lead to haploinsufficiency.

### Cas9 nuclease with paired gRNAs induce efficient editing at sites of the paracentric inversion

To assess the potential of Cas9 nucleases with paired gRNA for correcting the pathogenic inversion in patient-derived fibroblasts (Figures 2A and 2B), we designed gRNAs that specifically target the junction sites between fragment A and the inverted B (13 kb) fragment, as well as between the inverted B (13 kb) and C fragments (Figure 2C). We transfected patient fibroblast cells with complexes of Cas9 protein and *in vitro* transcribed gRNAs targeting the fragment junctions (Figure 2C), and measured editing frequencies using targeted deep sequencing (Figure 2D). The editing efficiency at target sites AB-T1 and AB-T2, located at the junction between fragment A and the inverted B (13 kb) fragment (A-B junction), were found to be 36.9% and 1.9%, respectively. Similarly, the Cas9 nuclease targeting the junctions between the inverted B (13 kb) fragment and fragment C (B-C junction) at sites BC-T1, BC-T2, and BC-T3 showed editing efficiencies of 57.2%, 89.0%, and 78.6%, respectively. Based on these results, we selected Cas9 nucleases targeting either AB-T1 and BC-T2 or AB-T1 and BC-T3 to induce the correction of the pathogenic inversion.

We next investigated whether Cas9 nuclease with paired gRNAs could correct the pathogenic inversion between endogenous loci in patient-derived fibroblasts (Figure 2A). To induce a paracentric inversion between the A-B junction and B-C junction, we co-transfected Cas9 protein and paired gRNAs targeting the two junctions. We then amplified the expected inversion junctions with paracentric inversion-specific primer pairs and found that inversions were induced in cells transfected with Cas9 protein and paired gRNAs (Figure 2E). To further analyze these amplicons, we performed targeted deep sequencing and found that Cas9 nuclease could induce a



paracentric inversion that corrects the pathogenic inversion with additional small insertions or deletions (indels) at the junctions in patient-derived fibroblast cells (Figure 2F). Cas9 protein and paired gRNAs could induce not only inversion, but also large deletion. To measure the inversion and large deletion frequencies induced by Cas9 nuclease and paired gRNAs, we used dilution PCR.<sup>7,18</sup> Through this analysis, we found that using Cas9 nuclease and paired gRNAs in patient-derived fibroblast cells resulted in inversion frequencies of up to 1.6% and large deletion frequencies of up to 2.2% (Figures 2G and S4). These results demonstrate that Cas9 nuclease and paired gRNAs, which are specific to the patient's genome, can correct the pathogenic inversions with relatively high efficiency in patient-derived fibroblasts.

We next investigated the specificity of the Cas9 nuclease with paired gRNAs targeting AB-T1, BC-T2, and BC-T3 using multiplex Digenome-seq, a method that allows unbiased assessment of potential off-target sites.<sup>19,20</sup> Using multiplex Digenome-seq of patient fibroblast-derived gDNA, we found potential off-target sites that were cleaved by the Cas9 nuclease and validated by targeted amplicon sequencing. Of the 18 putative off-target sites identified, only one

(OFF6 associated with BC-T2 and located within an intronic region) was conclusively validated by targeted deep sequencing at a frequency of 1.0% (Figure 2H). These results confirm that paired Cas9 nuclease-mediated inversion is a highly specific method with minimal off-target effects.

#### Cas9 nuclease with paired gRNAs restores EYA1 expression and transcriptional activity

To verify that the genome editing elicited a recovery of the EYA1 transcript, we conducted qRT-PCR with a primer set that covered the breakpoint junctions (Table S3). Targeting both combinations of sites (AB-T1 with BC-T2 and AB-T1 with BC-T3) led to a significant increase in the amount of wild-type EYA1 transcripts (Figure 3A). The recovery of the EYA1 transcript can also be confirmed at the protein level; AB-T1 and BC-T2 treatments induced a 1.3-fold increase in EYA1 protein levels, and AB-T1 and BC-T3 treatments resulted in a 1.4-fold increase (Figure 3B). To assess the potential restoration of the EYA1 transcriptional activity, we used a luciferase assay (Figure 3C). EYA1 encodes a transcriptional coactivator; the Eya domain is crucial for the formation of the EYA1-SIX1-DNA complex that regulates the transcription of target genes involved in the development of the

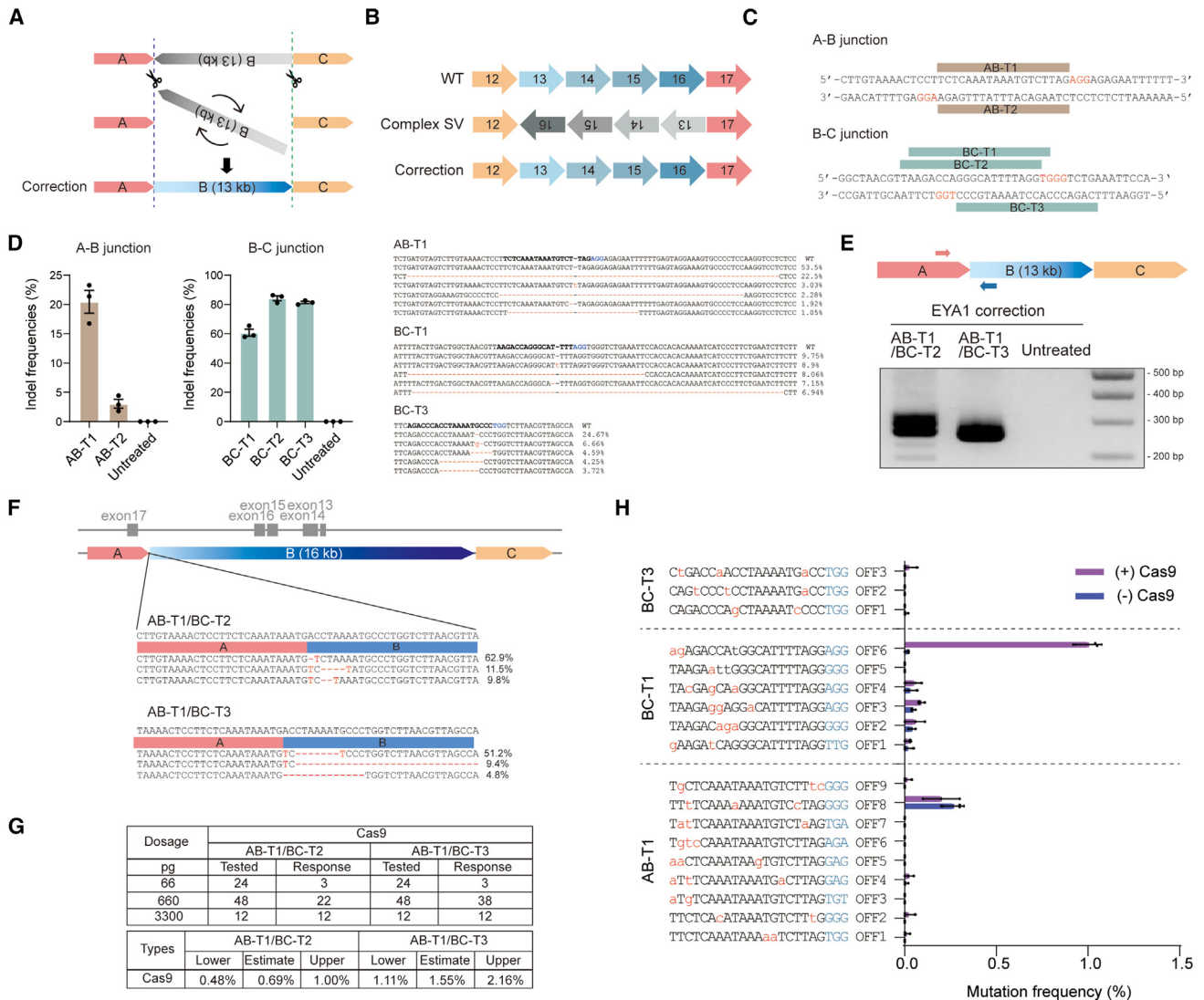


**Figure 2. Dual Cas9 nuclease-mediated correction of *EYA1* pathogenic complex**

(A) Schematic representation of Cas9 nuclease and paired gRNA-mediated correction of the pathogenic inversion. The dashed lines represent the Cas9 target sites. (B) Schematic representation of the mature mRNA anticipated after correction of the pathogenic inversion. (C) The Cas9 target sequences at the A-B junction and B-C junction of the pathogenic *EYA1* gene in patient fibroblasts. The protospacer adjacent motif is highlighted in red. (D) Mutation frequencies induced by Cas9 nuclease at the A-B junction and B-C junction of the *EYA1* gene. Data are presented as the mean  $\pm$  SD ( $n = 3$ ). (E) Detection of Cas9 nuclease-mediated inversions using inversion-specific primers. (F) Targeted deep sequencing reads of amplicons generated using inversion-specific primers. (G) Estimation of inversion frequencies by digital PCR analysis using serially diluted samples. Diluted genomic DNA samples were subjected to PCR using inversion-specific primers. The results were analyzed using the Extreme Limiting Dilution Analysis program (<http://bioinf.wehi.edu.au/software/elda/>). (H) Mutation frequencies at the off-target sites obtained by Digenome-seq analysis. Data are presented as the mean  $\pm$  SD ( $n = 3$ ).

branchial arch, otic system, and renal system.<sup>21</sup> In this context, we used the pGL4.12[luc2CP]-MYOG-6xMEF3 construct, which incorporates a luciferase reporter along with six repeats of the MEF3 motif. Importantly, each motif exhibits a specific affinity for the *EYA1* and *SIX1* protein complex. Under the conditions of *SIX1* overexpression, we observed that the luciferase activity in the *EYA1* CGR significantly decreased to 12.7% of the wild-type levels, representing a 7.8-fold decrease. In contrast, edited cells displayed a substantial increase in

luciferase activity relative to the mutant, with increases of 2.7-fold at the AB-T1 and BC-T2 sites, and 3.4-fold at the AB-T1 and BC-T3 sites. These values represent 34.1% and 43.8%, respectively, of the luciferase activity levels measured in the control cells. Furthermore, this gene editing was associated with a beneficial effect on the transcriptional activity of *EYA1*, as evidenced by the restoration of expression for several downstream target genes, including *SOX2*, *GFI1*, *ATOH1*, and *NEUROG1*. These genes are crucial for auditory

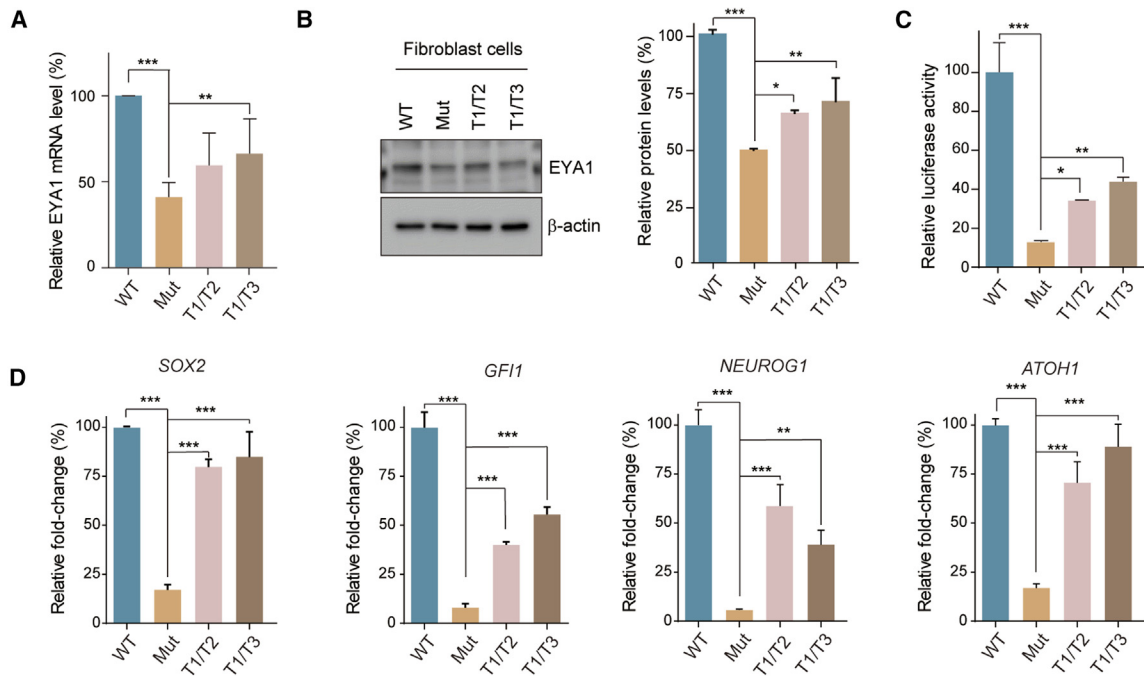


**Figure 3. Restoration of *EYA1* gene expression**

(A) Wild-type *EYA1* transcript levels in both patient-derived and edited fibroblast cells. qRT-PCR analysis was performed, and the *GAPDH* mRNA levels were used to normalize the levels of *EYA1* expression. Each bar represents the means of percent values (relative to the *EYA1* mRNA levels in wild-type fibroblast cells)  $\pm$  SD from three independent experiments. \* $p < 0.05$ ; \*\* $p < 0.01$  ( $n = 3$ , one-way ANOVA followed by Bonferroni's multiple comparison test). (B) (Left) *EYA1* protein levels were analyzed using SDS-PAGE followed by immunoblotting. (Right) For quantification, *EYA1* signal intensities were normalized to those of beta-actin. Images were processed with ImageJ to be quantified. Bars represent the mean  $\pm$  SD. \* $p < 0.05$ , \*\* $p < 0.01$ , \*\*\* $p < 0.001$  ( $n = 3$ , one-way ANOVA followed by Bonferroni's multiple comparison test). (C) Fibroblast cells were concurrently transfected with an *MYOG* promoter-driven luciferase reporter and the *SIX1* wild-type construct. Relative luciferase activity (wild-type as control) was plotted as mean  $\pm$  SD ( $n = 3$ ). \* $p < 0.05$ , \*\* $p < 0.01$ , \*\*\* $p < 0.001$  (one-way ANOVA followed by Bonferroni's multiple comparison test). (D) Total RNA was isolated, and the target genes (*SOX2*, *GF11*, *NEUROG1*, and *ATOH1*) of *EYA1* were analyzed by qRT-PCR. *GAPDH* mRNA levels were used to normalize the results. Values are represented as the mean  $\pm$  SD of three independent experiments ( $n = 3$ ). \* $p < 0.05$ , \*\* $p < 0.01$ , \*\*\* $p < 0.001$  ( $n = 3$ , one-way ANOVA with Bonferroni's multiple comparison test).

and neural development<sup>22,23</sup> (Figure 3D). Collectively, our data suggest that the Cas9 nuclease and paired gRNAs, designed to specifically target the paracentric inversion in the patient genome, are capable of restoring the transcriptional functionality of *EYA1*.

In the literature, *EYA1* CGRs involving inversions and deletions have been well-documented in BOR/BO cases.<sup>24,25</sup> Consistent with this, our in-house database revealed that two unrelated BOR/BO families were segregated with CGRs (Figure S2), including a cryptic large inversion (Table S4). Thus, the dual CRISPR-Cas9 system developed herein has the potential to correct pathogenic SVs, including those with *EYA1* CGRs, implicated in human genetic disorders.

#### Development of *EYA1* CRISPRa for haploinsufficiency

The pathological inversion in *EYA1* was anticipated to induce NMD, leading to haploinsufficiency (Figures 1D and 3A). To verify this, cells were treated with CHX, a well-established inhibitor of NMD. The treatment led to the stabilization of *EYA1* mRNA, suggesting that the haploinsufficiency linked to *EYA1* is dependent on the NMD pathway (Figure 4A). To investigate the potential of CRISPRa for inducing increased endogenous *EYA1* expression, we transfected

plasmid DNA encoding dSaCas9-VP64 and gRNA targeting the *EYA1* promoter into HEK293T cells and compared the relative expression of *EYA1* mRNA in treated cells and control cells (Figure 4B). Using qRT-PCR, we observed that dSaCas9-VP64 led to a substantial 4.0-fold upregulation of *EYA1* mRNA expression compared with untreated HEK293T cells. To model the potential haploinsufficiency originating from a variety of mechanisms and to evaluate the performance of the CRISPRa, we engineered HEK293T cells with either monoallelic or biallelic knockouts of *EYA1* (Figure 4C). We then investigated whether co-expressing dSaCas9-VP64 with either gRNA2 or 3 affected the mRNA expression of *EYA1* in these cell lines. Quantitative assessments of relative mRNA abundances indicated marked increases in wild-type and monoallelic knockout cells, with up to 3.7- and 1.4-fold increases, respectively, when compared with untreated cells. In contrast, cells with biallelic knockouts exhibited no discernible alterations in mRNA levels (Figure 4D). In addition, we transfected dSaCas9-VP64 with the corresponding gRNA in patient fibroblast cells and observed that dSaCas9-VP64 led to a 1.5-fold and 1.9-fold upregulation of *EYA1* mRNA expression, respectively, compared with untreated patient fibroblast cells (Figure 4E). We further analyzed transcriptional

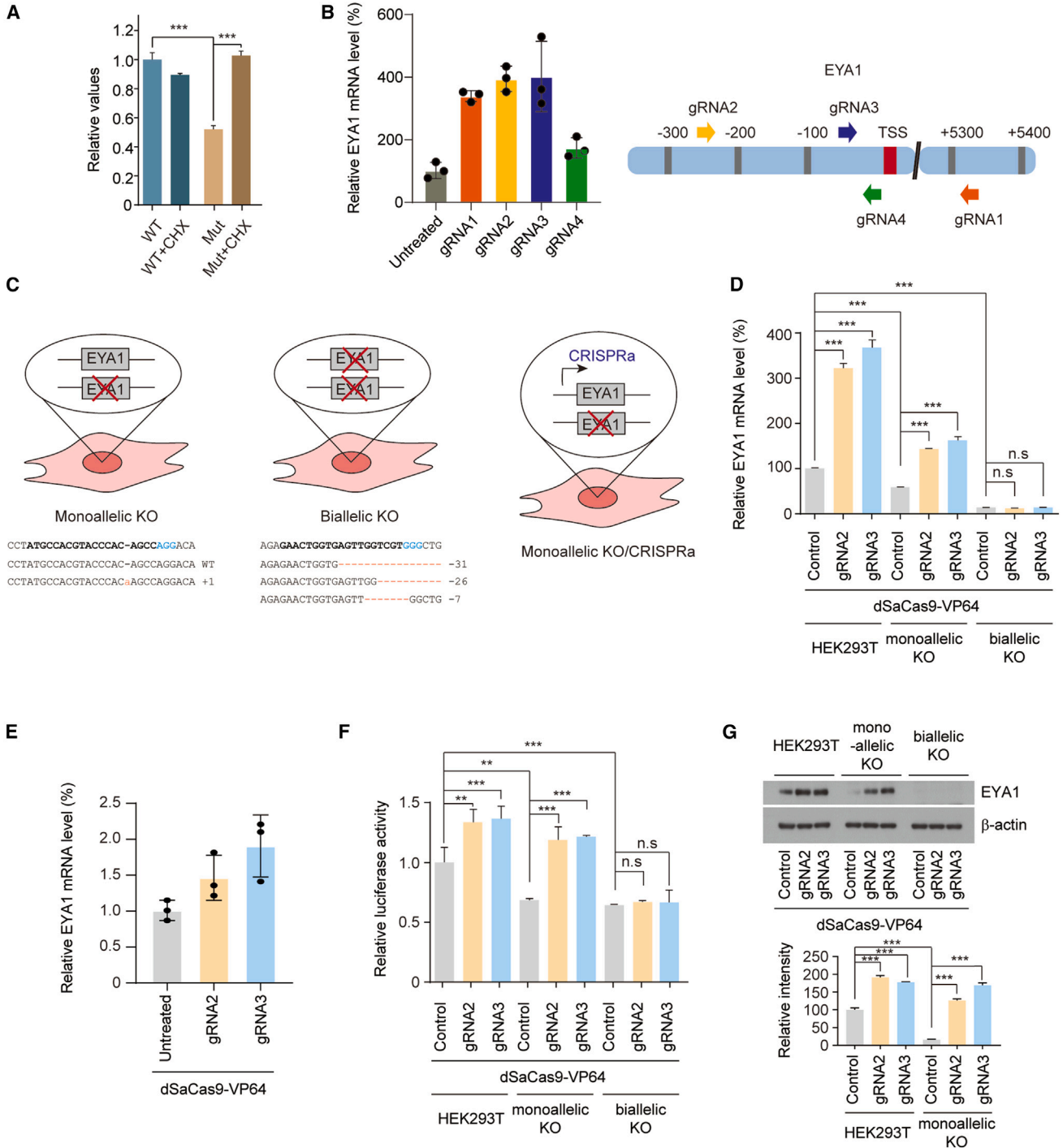


**Figure 4. Designing a CRISPRa strategy to elevate EYA1 levels**

(A) Relative EYA1 transcript levels were determined by qRT-PCR. Fibroblast cells were treated with DMSO or CHX (50  $\mu$ g/mL) for 6 h. All values were normalized to the untreated wild-type cells data and plotted as mean  $\pm$  SD ( $n = 3$ ).  $***p < 0.001$  (one-way ANOVA followed by Bonferroni's multiple comparison test). (B) (Left) HEK293T cells were transfected with CRISPRa plasmid. Subsequently, qRT-PCR was used to assess the expression of EYA1, and normalized to the expressions of the GAPDH housekeeping gene. Data are presented as the mean  $\pm$  SD ( $n = 3$ ). (Right) Graphical depiction of EYA1 gene's promoter region, including transcription start sites (TSSs). gRNA1–gRNA4 represent target sites of CRISPRa. (C) Schematic representation of monoallelic and biallelic EYA1 knockout cells with their genotypes. EYA1

(legend continued on next page)

activity of *EYA1* through a luciferase-based reporter gene assay, aiming to assess the potential restoration of *EYA1* functionality with CRISPRa (Figure 4F). Under untreated conditions, the luciferase activity in both monoallelic and biallelic knockout cells showed substantial reductions, by 68.5% and 64.4%, respectively, compared with HEK293T cells. Conversely, cells subjected to CRISPRa had enhanced luminescence, with increases of 1.3-fold in HEK293 cells and 1.7-fold in monoallelic knockout cells relative to their untreated counterparts. Consistent with the results of mRNA levels, biallelic knockout cells were not affected by CRISPRa. In line with these observations, protein levels in CRISPRa-treated cells increased by 1.84-fold in HEK293T cells and 8.00-fold in monoallelic knockout cells (Figure 4G). Given that monoallelic knockout cells displayed approximately 30% of the *EYA1* protein levels relative to their wild-type in normal conditions, we proceeded to treat these cells with MG132, a specific proteasome inhibitor, to investigate the potential role of proteolytic pathways in the modulation of *EYA1* protein levels (Figure S5). This treatment effectively stabilized *EYA1* protein levels, bringing the ratio between wild-type and monoallelic knockout cells to close to 50%. These observations lead us to hypothesize that proteasomal degradation may play a pivotal role in the haploinsufficiency observed with *EYA1* CGR in conjunction with NMD.

In the ClinVar database (<https://www.ncbi.nlm.nih.gov/clinvar/>), we noted that 81 disease-causing *EYA1* variants (pathogenic or likely pathogenic) were implicated in BOR/BO syndrome (Figure 5A; Table S5). The majority (68%) of the documented *EYA1* variants with BOR/BO phenotypes were loss-of-function, including nonsense, frameshift, canonical splicing, and SVs, resulting in haploinsufficiency (Figure 5B). Our results indicate that CRISPRa holds potential as a versatile genome editing approach to address *EYA1* haploinsufficiency, including those involving CGRs, suggesting its significance for personalized genome-specific interventions. In addition, based on human genetics databases, we found no evidence of pathogenic, disease-causing overexpression of *EYA1* (e.g., gain or amplification in dosage) linked with human phenotypes.

## DISCUSSION

This study highlights the importance of SVs, including CGRs and inversions, in rare disease.<sup>1,26</sup> In the literature, various genomic rearrangements, such as cryptic inversions and large deletions, have been well documented in approximately 20% of BOR/BO cases.<sup>14,24</sup> In certain cases, not only *EYA1* but also other genes were found to be involved, resulting in BOR/BO syndrome with additional clinical phenotypes.<sup>14</sup> Furthermore, non-allelic homologous recombination

and human endogenous retrovirus elements are known to induce recurrent genomic rearrangements associated with BOR/BO syndrome.<sup>27,28</sup> The advancement of genomic technologies, coupled with lower sequencing costs and improved data management, has made extraordinary strides toward deciphering the complex genetic architecture underlying human genetic disorder.<sup>1,29</sup> In parallel with this, precision genome editing approaches tailored to the patient's genome facilitate the recovery of transcriptional activity vital for target gene expression. Therefore, we believe that the dual CRISPR-Cas9 system or CRISPRa-based gene therapy could have the potential to expand the treatment landscape for human genetic disorders, even for pathogenic SVs and CGRs. However, these preclinical *in vitro* studies also need to be tested in *in vivo* models to verify efficacy and ensure safety before transitioning to clinical trials.

Previous studies have shown the potential of targeted gene addition strategies as a therapeutic approach for hemophilia A, which is often caused by pathogenic inversions of the *F8* gene.<sup>30</sup> This approach led to the restoration of *F8* expression in mesenchymal stem cells and endothelial cells, which had been differentiated from gene-corrected induced pluripotent stem cells.<sup>30</sup> Moreover, Hu et al.<sup>31</sup> provided a gene correction strategy for hemophilia A, caused by an *F8* intron 1 large sequence inversion variant, through homology-mediated end joining with a high efficiency of 10.2%.<sup>31</sup> Genome editing using paired gRNAs has demonstrated efficient genomic modifications across various preclinical studies and even extended to human trials in the treatment of ophthalmic diseases.<sup>32,33</sup> The human trial used paired gRNAs to target and delete the aberrant splice donor site caused by the *CEP290* variant, which is commonly associated with Leber congenital amaurosis type 10, suggesting the potential of a Cas9 nuclease and paired gRNA system for therapeutic genome editing in human genetic disorders.<sup>32</sup> Furthermore, prime editing approaches that use paired pegRNAs<sup>34</sup> and prime editor nuclease-mediated translocation and inversion<sup>7</sup> can facilitate programmable genome editing in mammalian cells. These approaches utilize paired pegRNAs oriented in a protospacer adjacent motif—in configuration to structure 3' flaps on opposing genetic strands. These strategies demonstrate variances in both the synthesized flaps and the approaches used for DNA target incision.<sup>34</sup> Although CRISPR-based genome editing technologies to correct inversion sequences are evolving, there is a lack of published evidence on the therapeutic potential of Cas9 nuclease with paired gRNAs to target disease-causing paracentric inversions in patient-derived cells.

Cas9-derived DNA DSBs at dual loci within the *EYA1* gene have the potential to catalyze genomic rearrangements, as demonstrated by the

---

haploinsufficiency was rescued using CRISPRa. (D) As in (B), except that dSaCas9-VP64 and either gRNA 2 or 3 were expressed in monoallelic and biallelic *EYA1* knockout HEK293T cells, as well as wild-type HEK293T cells. Values represent relative mRNA levels compared with HEK293 cells without transfection (control). \*\*\* $p < 0.01$  ( $n = 3$ , one-way ANOVA followed by Bonferroni's multiple comparison test). (E) dSaCas9-VP64 mediated relative *EYA1* mRNA expression in patient-derived fibroblasts. (F) The *MYOG* promoter-driven luciferase reporter and the *SIX1* wild-type construct were introduced into HEK293T cells and variants with either monoallelic or biallelic *EYA1* knockouts. Relative luciferase activity (relative to the HEK293T control) is plotted as mean  $\pm$  SD ( $n = 3$ ). \* $p < 0.05$ , \*\* $p < 0.01$  (one-way ANOVA followed by Bonferroni's multiple comparison test). (G) As in (D), except that whole cell extracts were subjected to SDS-PAGE followed by immunoblotting (top). For quantification (bottom), signals from *EYA1* were normalized to those of beta-actin. Images were processed with ImageJ to be quantified. Bars represent the mean  $\pm$  SD. \*\*\*,  $p < 0.001$  ( $n = 3$ , one-way ANOVA followed by Bonferroni's multiple comparison test).

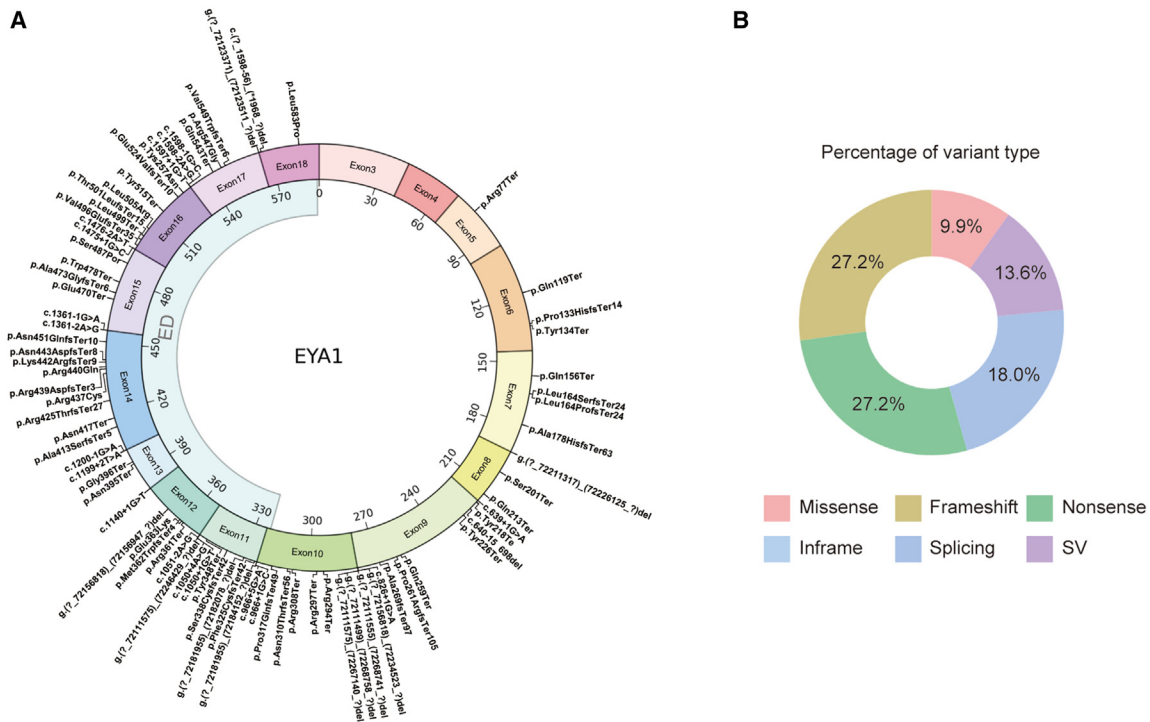


**Figure 5. Genomic landscape of disease-causing *EYA1* variants implicated in BOR/BO syndrome**

(A) Circos plot ([https://github.com/SNUH-hEARgeneLab/WGS\\_analysis](https://github.com/SNUH-hEARgeneLab/WGS_analysis)) illustrating the distribution of all reported disease-causing *EYA1* variants from the ClinVar database. On the outer domain, the *EYA1* exons and corresponding reported variants are depicted, while the inner domain displays the EYA domain (ED) of *EYA1*. (B) Pie chart demonstrating the percentage of each variant type of *EYA1* disease-causing variants associated with BOR/BO syndrome.

paracentric inversion editing event in this study. Mechanistically, the CRISPR-Cas9 system, when used with paired gRNAs designed to target distinct genomic locations, has the potential to yield diverse modifications in DNA.<sup>35,36</sup> The inversion generated by a dual CRISPR-Cas9 system has been demonstrated across mammalian cell lines,<sup>8,37</sup> as well as *in vivo* in animal models,<sup>38</sup> suggesting the validity of the system in engineering specific inversion mutations. Although indels occur due to the Cas9 nuclease targeting *EYA1* (Figure 2F), it is thought that their occurrence may not be significantly important, as they are located in the intron regions. Encouraged by these insights, we hypothesize that paired gRNAs could be a potential therapeutic option to correct the disease-causing CGRs implicated in BOR/BO syndrome. We successfully applied the dual CRISPR-Cas9 system that specifically targeted a disease-causing paracentric inversion in patient-derived cells. The system demonstrated the significant editing efficiency, leading to the restoration of gene expression and associated transcriptional functionality. Considering that an editing efficiency of even 1%–2% in primary cells using CRISPR-Cas9 nuclease has been shown to rescue the hearing function of mice with *Atp2b2* variants,<sup>39</sup> the 1.6% editing efficiency we achieved in patient-derived fibroblasts is particularly noteworthy. The relationship between genomic editing efficiency and phenotypic recovery is intricate and not strictly linear. Considering the NMD pathway's influence linked to haploinsufficiency, the 1.6% genomic correction observed in our study may lead to a disproportionately large recovery of *EYA1*'s

transcriptional and translational activity. This phenomenon is consistent with observations from other *in vivo* gene editing studies, such as the correction of the predicted loss-of-function mutant alleles resulting in NMD, where a modest DNA edit led to a much higher mRNA edit associated with phenotypic and functional restorations.<sup>40,41</sup> This result raises the possibility of restoring disease phenotypes, such as hearing impairment, in BOR/BO patients with *EYA1* CGRs, including paracentric inversion.

CRISPRa utilizes a Cas9 variant, dCas9, which lacks nuclease activity, combined with a transcriptional activator. By targeting the *EYA1* promoter, the dCas9-VP64 fusion used in our CRISPRa system increases *EYA1* expression (see Figure 4B), leading to significantly improved transcriptional activity essential for target gene expression. Of the documented *EYA1* variants linked with BOR/BO phenotypes, approximately 70% are described as monoallelic loss-of-function variants, including nonsense, frameshift, canonical splicing, and SVs (see Figure 5B). As a consequence, there is a state of haploinsufficiency. This suggests that CRISPRa-based gene therapies may offer substantial translational potential for approximately 70% of disease-causing *EYA1* variants caused by haploinsufficiency.

Gene therapies (e.g., gene transfer or augmentation) have revolutionized the treatment landscape for human genetic disorders. However, despite their substantial clinical benefits, these therapies are met with

challenges associated with the long-term durability of therapeutic efficacy. The repeated viral delivery-based gene therapy may increase the risk of viral vector integration into the genome of transduced cells, potentially increasing the oncogenesis.<sup>42,43</sup> Furthermore, the emergence of neutralizing antibodies following the viral delivery may compromise treatment effectiveness.<sup>44</sup> In light of these challenges, the development and refinement of CRISPR-Cas9 technology can offer precise genome editing capabilities that have shown promising results in both basic and clinical research for the treatment of various genetic conditions, including  $\beta$ -thalassemia.<sup>45</sup> Additionally, the advent of CRISPR-based methodologies that do not require DNA DSBs, such as base editing and prime editing, are on the way to clinics.<sup>46</sup> Our findings cannot ascertain a definitive superiority between CRISPR-guided genome editing and additive gene therapy for treating pathogenic SVs. While conventional gene therapy may prove effective in cases of haploinsufficiency linked to *EYA1* CGR, as demonstrated herein, we emphasize that CRISPR-guided genome editing tailored to the patient's genome, including Cas9 nuclease and paired gRNAs and CRISPRa, also offers a viable approach to rectify pathogenic SVs. *EYA1* produces three isoforms through alternative splicing, which can pose challenges for gene transfer strategies. However, CRISPR-guided genome editing and CRISPRa affected endogenous gene expression, potentially inducing the expression of all isoforms. This offers a comprehensive solution for the complexity introduced by multiple isoforms. Meanwhile, for genetic diseases caused by missense mutations, such as those resulting in mutant proteins, gene editing is likely to be more advantageous compared with additive gene therapy. This is because gene editing circumvents the uncertainties associated with interactions between delivered wild-type transgenes and mutant alleles, which can be problematic in disease phenotypes. For example, the ineffectiveness of wild-type p53 gene therapy can be attributed to the dominant negative effect, where mutant p53 proteins in cancer cells bind with the introduced wild-type p53, leading to the formation of non-functional heterotetramers that fail to activate crucial tumor suppressor functions.<sup>47</sup>

In conclusion, our results pave the way for the potential development of gene editing therapeutics for the clinical application of human genetic disorders caused by pathogenic SVs such as inversion and genomic rearrangements. In particular, BOR/BO syndrome stands as a representative case where hearing impairment is the most penetrant symptom.<sup>11,13</sup> Most branchial anomalies associated with this syndrome can be managed surgically, and the renal phenotype is rare. *EYA1* plays a crucial role in the development of the ear, supporting the patterning of the otocyst and mediating the specification of the prosensory region. Given this, its influence extends beyond the inner ear to the middle and outer ears, which are important for sound conduction. Therefore, the auditory phenotypes of patients with *EYA1* pathogenic variants often present as mixed hearing loss, including both sensorineural and conductive components. According to the hearing loss phenotypes in patients with BOR/BO syndrome,<sup>11,13</sup> the SNHL component is often observed to be less severe than expected. Issues related to the middle and outer ear, which contribute to the conductive hearing loss (e.g., air-bone gap), can be significantly improved through middle ear sur-

geries, such as ossiculoplasty and stapedotomy.<sup>11</sup> While improvements in the already compromised sensory epithelium during inner ear development are limited by gene editing, the deterioration of SNHL linked to reduced transcriptional activity due to *EYA1* variants holds promising potential for intervention using CRISPR-guided therapies. Although *in vivo* AAV-mediated Cas9 expression can induce humoral and cellular immune responses,<sup>48</sup> the inner ear presents a particularly promising target for gene therapy due to its low immunogenicity. AAV-mediated inner ear gene delivery does not trigger significant local or systemic cellular immune activation, and its compact, enclosed structure facilitates localized intervention. Previous studies have highlighted the efficacy of adeno-associated viruses (AAVs) in transducing overexpressed cDNA and gene editing materials into target cells within the inner ear.<sup>40,49</sup> The advancements in gene editing technologies, including dual CRISPR-Cas9 system and CRISPRa with AAV-mediated sustained expression, could expand the therapeutic landscape related to human genetic disorders, and encompass conditions such as BOR/BO syndrome due to *EYA1* CGRs associated with haploinsufficiency.

## MATERIALS AND METHODS

### Participants

All procedures were approved by the Institutional Review Board of Seoul National University Hospital (IRB-H-0905-041-281 and IRB-H-2202-045-1298). In this study, one BOR/BO multiplex family segregated with CGR was included in the Hereditary Hearing Loss Clinic within the Otorhinolaryngology division of the Center for Rare Diseases, Seoul National University Hospital, Korea. The demographic data and clinical phenotypes were retrieved from electronic medical records. The presence and severity of associated medical conditions were determined using the Tenth Revision of the *International Statistical Classification of Diseases and Related Health Problems* codes and/or features in their clinical manifestations.

### Whole-exome sequencing and MLPA

Genomic DNA was extracted from peripheral blood samples and used in whole-exome sequencing via SureSelectXT Human All Exon V5 (Agilent Technologies, Santa Clara, CA, USA). Adhering to the instructions provided, we prepared a library which was then sequenced using a NovaSeq 6000 system (Illumina, San Diego, CA, USA) in a paired-end manner. Sequence reads were compared with the human reference genome (GRCh38) and processed in line with the Genome Analysis Toolkit best-practice guidelines to identify single nucleotide variants (SNVs) and indels.<sup>50</sup> The ANNOVAR program was used for variant annotation, such as from the RefSeq gene set and gnomAD.<sup>51,52</sup> Rare non-silent variants were selected as candidates, including nonsynonymous SNVs, coding indels, and splicing variants. We also used the KRGDB and KOVA databases for further filtration of ethnic-specific variants.<sup>53,54</sup> We conducted a comprehensive bioinformatics analysis to detect candidate variants using a defined filtering process, as described previously.<sup>11,55,56</sup>

We also assessed the copy number status of *EYA1* using a SALSA MLPA P461 DIS Probemix kit (MRC-Holland, Amsterdam, THE

Netherlands). The amplification products were analyzed with an ABI PRISM 3130 Genetic Analyzer (Applied Biosystems, Foster City, CA, USA), and the results were interpreted with the aid of Gene Marker 1.91 software (SoftGenetics, State College, PA, USA).

### WGS and bioinformatics

Genomic DNA was extracted from peripheral blood samples using Allprep DNA/RNA kits (Qiagen, Venlo, the Netherlands) and libraries were generated with TruSeq DNA PCR-Free Library Prep Kits (Illumina). The libraries were then sequenced on the Illumina NovaSeq6000 platform with the coverage set at an average depth of 30×. The obtained sequences were aligned to the human reference genome (GRCh38) using the BWA-MEM algorithm and PCR duplicates were eliminated using SAMBLASTER. Mutation calling for base substitutions and short indels was achieved with HaplotypeCaller2 and Strelka2, respectively. Delly was used to identify SVs. The breakpoints of the genomic rearrangements of interest were visually examined and validated. Variant filtering and assessment of their Mendelian inheritance patterns were carried out. The pathogenicity of the variants was classified using the American College of Medical Genetics and Genomics/Association for Molecular Pathology guidelines.<sup>57</sup>

### Cell culture and transfection

Patient fibroblasts were maintained in DMEM supplemented with 10% fetal bovine serum and 1% penicillin/streptomycin/amphotericin. To induce the correction of pathogenic inversion,  $2 \times 10^5$  patient fibroblasts were transfected with 17 µg Cas9 protein, 5 µg *in vitro* transcribed gRNA targeting the A-B junction, and 5 µg *in vitro* transcribed gRNA targeting the B-C junction using an Amaxa P3 Cell Line 4D-Nucleofector Kit (CM-137 program). Cells were analyzed 3 days after transfection.

HEK293T cells (American Type Culture Collection, CRL-11268) were maintained in DMEM supplemented with 10% fetal bovine serum and 1% penicillin/streptomycin. For dCas9-VP64-mediated *EYA1* activation, HEK293T cells were seeded onto 24-well plates and transfected with 2,000 ng plasmid DNA encoding dSaCas9-VP64 and gRNA (Addgene plasmid #158990) using 3 µL Lipofectamine 2000 (Life Technologies, Carlsbad, CA, USA). After 72 h, total RNA was isolated with an RNeasy Mini Kit (Qiagen) according to the manufacturer's instructions.

### Targeted deep sequencing

Genomic DNA containing the on-target was amplified using KAPA HiFi HotStart DNA polymerase. The amplified products were designed to include Illumina TruSeq HT dual index adapter sequences. Subsequently, the amplified products were subjected to 150-bp paired-end sequencing using the Illumina iSeq 100 platform. To calculate the frequencies of indels, we used the MAUND tool, which is available at <https://github.com/ibs-cge/maund>.

### RNA isolation and real-time qPCR

Total RNA (1 µg) was extracted from either fibroblasts or HEK293T cells using the TRIzol method, with subsequent purification via

RNeasy mini-columns (Qiagen) and an incorporated on-column Dnase I treatment. The synthesis of cDNA was achieved from 2 µg of the isolated total RNA using the RT-PCR method and Accupower RT-pre-mix (Bioneer, Oakland, CA, USA). Quantitative RT-PCR assays were performed on cDNA samples diluted 1/20 using SYBR qPCR master mix (Kapa Biosystems, Wilmington, MA, USA) as the reporter dye. Primers at a concentration of 10 pM were used to detect specific gene mRNA expression. Their sequences were as follows: *SOX2*, forward 5'-GCTACAGCATGATGCAGGACCA-3' and reverse 5'-TCTGCGAGCTGGTTCATGGAGTT-3'; *NEUROG1*, forward 5'-GCCTCCGAAGACTTCACCTACC-3' and reverse 5'-GGA AAGTAACAGTGTCTACAAAGG-3'; *GFI1*, forward 5'-GCTTCAA GAGGTCATCCACACTG3' and reverse ACCTGGCACTTGTGAG GCTTCT-3'; and *GAPDH*, forward 5'-GAGTCAACGGATTTGGT CGT-3' and reverse 5'-GACAAGCTTCCCGTTCTCAG-3'. The primer sequences for *EYA1* can be found in the Supplementary Tables. The relative frequency of *EYA1* mRNA was determined using the comparative  $C_T$  method.<sup>58</sup>

### Luciferase reporter gene assay

The luciferase reporter gene assay was performed, as described previously with slight modifications.<sup>11</sup> Briefly, HEK293T cells were transfected initially with three distinct plasmids: pGL4.12[luc2CP]-MYOG-6xMEF3, pRK5-SIX1, and pRL/CMV (E2261, Promega, Madison, WI, USA). After transfection, the cells were harvested for a luciferase assay using a Dual-Luciferase Reporter Assay kit (E1910, Promega), following the manufacturer's guidelines. Transfection efficiency was adjusted based on Renilla activity, which was assessed after co-transfection with pRL/CMV.

### Statistical analysis

Statistical analyses were executed utilizing GraphPad Prism, version 10, to ensure rigorous data evaluation. For the comparative analysis involving multiple groups, we employed ANOVA, subsequently followed by Bonferroni's multiple comparison test for precise *p* value calculation. Throughout the analyses, we adhered to a strict threshold of  $p < 0.05$  to ascertain statistical significance, ensuring consistency and reliability in our findings.

### Generating single cell-derived *EYA1* knockout clones

HEK293T cells were maintained in DMEM supplemented with 10% fetal bovine serum and 1% penicillin-streptomycin. For the transfection, the cells were seeded in 24-well plates and co-transfected with 1,500 ng of the Cas9 expression plasmid and 500 ng of a single guide RNA (sgRNA)-encoding plasmid containing a spacer sequence (5'-ATGCCACGTACCCACAGCC-3' on the top strand and 5'-GGC TGTGGGTACGTGGCAT-3' on the bottom strand). Single-cell clones were generated via limiting dilutions in 96-well plates, followed by clonal expansion. Genomic DNA from these clones was isolated using Allprep DNA/RNA kits (Qiagen) according to the manufacturer's instructions, and mutation frequencies were determined through targeted deep sequencing.

### Immunoblotting

Cells were washed with PBS and lysed using RIPA buffer supplemented with protease inhibitors. The lysates combined with sample buffer were denatured at 85°C in preparation for SDS-PAGE. Subsequently, proteins were transferred to PVDF membranes. Membranes were blocked in 5% nonfat milk in TBS-T and then probed with primary antibodies. After comprehensive washing, membranes were exposed to horseradish peroxidase-linked secondary antibodies, specific to rabbit or mouse IgG. Protein bands became evident upon chemiluminescence application and were subsequently imaged. Band intensities were quantified using ImageJ software based on replicated experiments. Statistical evaluation was conducted using GraphPad Prism V5. Results with a *p* value of <0.05 were used to confirm significance. Sources of antibodies and working dilutions were as follows: beta-actin, anti-β-actin (A1978, Sigma, 1/10,000); anti-EYA1 (22658-1-AP, Proteintech [Rosemont, IL, USA], 1/1,000). For immunoblotting EYA1 in fibroblasts, the process begins with centrifuging patient-derived fibroblast cells for collection and washing them with PBS. The next step involves separating the nuclear and cytosolic fractions using the Subcellular Protein Fractionation Kit (Cat#78840, Thermo Fisher Scientific, Waltham, MA, USA), according to the instructions provided. To further enhance EYA1 detection in immunoblotting, the nuclear fractions are concentrated using Amicon Ultra-0.5 centrifugal filter units (Millipore, Burlington, MA, USA), ensuring a more effective analysis. This refined procedure is crucial for accurately assessing EYA1 expression.

### Digenome-seq

The genomic DNA was extracted using the DNeasy Tissue kit (Qiagen) following the manufacturer's protocol. SpCas9 nuclease, at a concentration of 100 mM, was combined with AB\_T1, BC\_T2, and BC\_T3 sgRNAs, each at a concentration of 100 nM, and the mixture was incubated at room temperature for 30 min. This mixture was then added to 10 μg of genomic DNA in a 1000ul reaction volume containing 100 mM NaCl, 50 mM MgCl<sub>2</sub>, and 100 μg/mL BSA. After incubating the reaction mixture at 37 °C for 8 h, the digested genomic DNA underwent a secondary purification step using the DNeasy Tissue kit (Qiagen). During this purification process, RNase A (50 μg/mL) was added to remove any residual sgRNA. Cas9-mediated digested genomic DNA was subjected to WGS with a sequencing depth of 30×–40× using an Illumina Hi-Seq X Ten Sequencer at Macrogen. The genome sequence was mapped using the Isaac aligner and DNA cleavage sites were identified using the Digenome program, which is available at <https://github.com/chizksh/digenome-toolkit2>.

### DATA AND CODE AVAILABILITY

NGS data have been deposited at SRA under accession no. PRJNA1088183.

### SUPPLEMENTAL INFORMATION

Supplemental information can be found online at <https://doi.org/10.1016/j.omtn.2024.102199>.

### ACKNOWLEDGMENTS

This research was supported and funded by SNUH Kun-hee Lee Child Cancer & Rare Disease Project, Republic of Korea (FP-2022-00001-004 to S.-Y.L.), National Research Foundation of Korea (NRF) and funded by the Ministry of Education (grant number: 2022R1C1C1003147 to S.-Y.L.), SNUH Research Fund (04-2022-4010 to S.-Y.L. and 04-2022-3070 to S.-Y.L.), National Research Foundation of Korea (2020R1A2C2101714 to D.K.), Korean Fund for Regenerative Medicine (KFRM) grant funded by the Korean government (Ministry of Science and ICT, Ministry of Health & Welfare [21A0202L1-12 to D.K.]), and Korea Health Technology R&D Project through the Korea Health Industry Development Institute (KHIDI), funded by the Ministry of Health and Welfare, Republic of Korea (HI21C1314 and HR22C1363 to D.K.).

### AUTHOR CONTRIBUTIONS

S.-Y.L. and D.K. supervised the research. H.Y., Y.Y., W.H.C., H.-Y.H., and J.H.C. performed the experiments. H.S., J.-J.S, J.H.L., and S.-Y.L. carried out bioinformatics analyses. H.Y., Y.Y., W.H.C., H.-Y.H., S.-Y.L., and D.K. wrote the manuscript. All authors approved the manuscript.

### DECLARATION OF INTERESTS

The authors declare that they have no competing interests.

### REFERENCES

- Schuy, J., Grochowski, C.M., Carvalho, C.M.B., and Lindstrand, A. (2022). Complex genomic rearrangements: an underestimated cause of rare diseases. *Trends Genet.* 38, 1134–1146.
- Eijk-Van Os, P.G.C., and Schouten, J.P. (2011). Multiplex Ligation-dependent Probe Amplification (MLPA(R)) for the detection of copy number variation in genomic sequences. *Methods Mol. Biol.* 688, 97–126.
- Li, Y., Zheng, H., Luo, R., Wu, H., Zhu, H., Li, R., Cao, H., Wu, B., Huang, S., Shao, H., et al. (2011). Structural variation in two human genomes mapped at single-nucleotide resolution by whole genome de novo assembly. *Nat. Biotechnol.* 29, 723–730.
- Jinek, M., Chylinski, K., Fonfara, I., Hauer, M., Doudna, J.A., and Charpentier, E. (2012). A programmable dual-RNA-guided DNA endonuclease in adaptive bacterial immunity. *Science* 337, 816–821.
- Mali, P., Yang, L., Esvelt, K.M., Aach, J., Guell, M., DiCarlo, J.E., Norville, J.E., and Church, G.M. (2013). RNA-guided human genome engineering via Cas9. *Science* 339, 823–826.
- Zheng, Q., Cai, X., Tan, M.H., Schaffert, S., Arnold, C.P., Gong, X., Chen, C.Z., and Huang, S. (2014). Precise gene deletion and replacement using the CRISPR/Cas9 system in human cells. *Biotechniques* 57, 115–124.
- Kweon, J., Hwang, H.Y., Ryu, H., Jang, A.H., Kim, D., and Kim, Y. (2023). Targeted genomic translocations and inversions generated using a paired prime editing strategy. *Mol. Ther.* 31, 249–259.
- Choi, P.S., and Meyerson, M. (2014). Targeted genomic rearrangements using CRISPR/Cas technology. *Nat. Commun.* 5, 3728.
- Torres, R., Martin, M.C., Garcia, A., Cigudosa, J.C., Ramirez, J.C., and Rodriguez-Perales, S. (2014). Engineering human tumour-associated chromosomal translocations with the RNA-guided CRISPR-Cas9 system. *Nat. Commun.* 5, 3964.
- Ghezraoui, H., Piganeau, M., Renouf, B., Renaud, J.B., Sallmyr, A., Ruis, B., Oh, S., Tomkinson, A.E., Hendrickson, E.A., Giovannangeli, C., et al. (2014). Chromosomal translocations in human cells are generated by canonical nonhomologous end-joining. *Mol. Cell* 55, 829–842.
- Lee, S., Yun, Y., Cha, J.H., Han, J.H., Lee, D.H., Song, J.J., Park, M.K., Lee, J.H., Oh, S.H., Choi, B.Y., and Lee, S.Y. (2023). Phenotypic and molecular basis of SIX1 variants

- linked to non-syndromic deafness and atypical branchio-otic syndrome in South Korea. *Sci. Rep.* 13, 11776.
12. Masuda, M., Kanno, A., Nara, K., Mutai, H., Morisada, N., Iijima, K., Morimoto, N., Nakano, A., Sugiuchi, T., Okamoto, Y., et al. (2022). Phenotype-genotype correlation in patients with typical and atypical branchio-oto-renal syndrome. *Sci. Rep.* 12, 969.
  13. Nam, D.W., Kang, D.W., Lee, S.M., Park, M.K., Lee, J.H., Oh, S.H., Suh, M.W., and Lee, S.Y. (2023). Molecular Genetic Etiology and Revisiting the Middle Ear Surgery Outcomes of Branchio-Oto-Renal Syndrome: Experience in a Tertiary Referral Center. *Otol. Neurotol.* 44, e319–e327.
  14. Chang, E.H., Menezes, M., Meyer, N.C., Cucci, R.A., Vervoort, V.S., Schwartz, C.E., and Smith, R.J.H. (2004). Branchio-oto-renal syndrome: the mutation spectrum in EYA1 and its phenotypic consequences. *Hum. Mutat.* 23, 582–589.
  15. Feng, H., Xu, H., Chen, B., Sun, S., Zhai, R., Zeng, B., Tang, W., and Lu, W. (2021). Genetic and Phenotypic Variability in Chinese Patients With Branchio-Oto-Renal or Branchio-Oto Syndrome. *Front. Genet.* 12, 765433.
  16. Li, J., Cheng, C., Xu, J., Zhang, T., Tokat, B., Dolios, G., Ramakrishnan, A., Shen, L., Wang, R., and Xu, P.X. (2022). The transcriptional coactivator Eya1 exerts transcriptional repressive activity by interacting with REST corepressors and REST-binding sequences to maintain nephron progenitor identity. *Nucleic Acids Res.* 50, 10343–10359.
  17. Xu, P.X., Adams, J., Peters, H., Brown, M.C., Heaney, S., and Maas, R. (1999). Eya1-deficient mice lack ears and kidneys and show abnormal apoptosis of organ primordia. *Nat. Genet.* 23, 113–117.
  18. Lee, H.J., Kim, E., and Kim, J.S. (2010). Targeted chromosomal deletions in human cells using zinc finger nucleases. *Genome Res.* 20, 81–89.
  19. Kim, D., Kim, S., Kim, S., Park, J., and Kim, J.S. (2016). Genome-wide target specificities of CRISPR-Cas9 nucleases revealed by multiplex Digenome-seq. *Genome Res.* 26, 406–415.
  20. Kim, D., Bae, S., Park, J., Kim, E., Kim, S., Yu, H.R., Hwang, J., Kim, J.I., and Kim, J.S. (2015). Digenome-seq: genome-wide profiling of CRISPR-Cas9 off-target effects in human cells. *Nat. Methods* 12, 237–243.
  21. Ruf, R.G., Xu, P.X., Silvius, D., Otto, E.A., Beekmann, F., Muerb, U.T., Kumar, S., Neuhaus, T.J., Kemper, M.J., Raymond, R.M., Jr., et al. (2004). SIX1 mutations cause branchio-oto-renal syndrome by disruption of EYA1-SIX1-DNA complexes. *Proc. Natl. Acad. Sci. USA* 101, 8090–8095.
  22. Riddiford, N., and Schlosser, G. (2016). Dissecting the pre-placodal transcriptome to reveal presumptive direct targets of Six1 and Eya1 in cranial placodes. *Elife* 5, e17666.
  23. Ahmed, M., Xu, J., and Xu, P.X. (2012). EYA1 and SIX1 drive the neuronal developmental program in cooperation with the SWI/SNF chromatin-remodeling complex and SOX2 in the mammalian inner ear. *Development* 139, 1965–1977.
  24. Vervoort, V.S., Smith, R.J.H., O'Brien, J., Schroer, R., Abbott, A., Stevenson, R.E., and Schwartz, C.E. (2002). Genomic rearrangements of EYA1 account for a large fraction of families with BOR syndrome. *Eur. J. Hum. Genet.* 10, 757–766.
  25. Schmidt, T., Bierhals, T., Kortüm, F., Bartels, I., Liehr, T., Burfeind, P., Shoukier, M., Frank, V., Bergmann, C., and Kutsche, K. (2014). Branchio-otic syndrome caused by a genomic rearrangement: clinical findings and molecular cytogenetic studies in a patient with a pericentric inversion of chromosome 8. *Cytogenet. Genome Res.* 142, 1–6.
  26. Li, Y., Roberts, N.D., Wala, J.A., Shapira, O., Schumacher, S.E., Kumar, K., Khurana, E., Waszak, S., Korbel, J.O., Haber, J.E., et al. (2020). Patterns of somatic structural variation in human cancer genomes. *Nature* 578, 112–121.
  27. Chen, X., Wang, J., Mitchell, E., Guo, J., Wang, L., Zhang, Y., Hodge, J.C., and Shen, Y. (2014). Recurrent 8q13.2-13.3 microdeletions associated with branchio-oto-renal syndrome are mediated by human endogenous retroviral (HERV) sequence blocks.  *BMC Med. Genet.* 15, 90.
  28. Sanchez-Valle, A., Wang, X., Potocki, L., Xia, Z., Kang, S.H.L., Carlin, M.E., Michel, D., Williams, P., Cabrera-Meza, G., Brundage, E.K., et al. (2010). HERV-mediated genomic rearrangement of EYA1 in an individual with branchio-oto-renal syndrome. *Am. J. Med. Genet.* 152A, 2854–2860.
  29. Turro, E., Astle, W.J., Megy, K., Gräf, S., Greene, D., Shamardina, O., Allen, H.L., Sanchis-Juan, A., Frontini, M., Thys, C., et al. (2020). Whole-genome sequencing of patients with rare diseases in a national health system. *Nature* 583, 96–102.
  30. Wu, Y., Hu, Z., Li, Z., Pang, J., Feng, M., Hu, X., Wang, X., Lin-Peng, S., Liu, B., Chen, F., et al. (2016). In situ genetic correction of F8 intron 22 inversion in hemophilia A patient-specific iPSCs. *Sci. Rep.* 6, 18865.
  31. Hu, Z., Wu, Y., Xiao, R., Zhao, J., Chen, Y., Wu, L., Zhou, M., and Liang, D. (2023). Correction of F8 intron 1 inversion in hemophilia A patient-specific iPSCs by CRISPR/Cas9 mediated gene editing. *Front. Genet.* 14, 1115831.
  32. Maeder, M.L., Stefanidakis, M., Wilson, C.J., Baral, R., Barrera, L.A., Bounoutas, G.S., Bumcrot, D., Chao, H., Ciulla, D.M., DaSilva, J.A., et al. (2019). Development of a gene-editing approach to restore vision loss in Leber congenital amaurosis type 10. *Nat. Med.* 25, 229–233.
  33. Editas Medicine, I. (2022). Single Ascending Dose Study in Participants With LCA10. Identifier NCT03872479. <https://www.clinicaltrials.gov/study/NCT03872479?cond=NCT03872479&rank=1>.
  34. Chen, P.J., and Liu, D.R. (2023). Prime editing for precise and highly versatile genome manipulation. *Nat. Rev. Genet.* 24, 161–177.
  35. Sander, J.D., and Joung, J.K. (2014). CRISPR-Cas systems for editing, regulating and targeting genomes. *Nat. Biotechnol.* 32, 347–355.
  36. Bothmer, A., Phadke, T., Barrera, L.A., Margulies, C.M., Lee, C.S., Buquicchio, F., Moss, S., Abdulkarim, H.S., Selleck, W., Jayaram, H., et al. (2017). Characterization of the interplay between DNA repair and CRISPR/Cas9-induced DNA lesions at an endogenous locus. *Nat. Commun.* 8, 13905.
  37. Li, Y., Park, A.I., Mou, H., Colpan, C., Bizhanova, A., Akama-Garren, E., Joshi, N., Hendrickson, E.A., Feldser, D., Yin, H., et al. (2015). A versatile reporter system for CRISPR-mediated chromosomal rearrangements. *Genome Biol.* 16, 111.
  38. Maddalo, D., Manchado, E., Concepcion, C.P., Bonetti, C., Vidigal, J.A., Han, Y.C., Ogdowski, P., Crippa, A., Rektman, N., de Stanchina, E., et al. (2014). In vivo engineering of oncogenic chromosomal rearrangements with the CRISPR/Cas9 system. *Nature* 516, 423–427.
  39. Tao, Y., Lamas, V., Du, W., Zhu, W., Li, Y., Whittaker, M.N., Zuris, J.A., Thompson, D.B., Rameshbabu, A.P., Shu, Y., et al. (2023). Treatment of monogenic and digenic dominant genetic hearing loss by CRISPR-Cas9 ribonucleoprotein delivery in vivo. *Nat. Commun.* 14, 4928.
  40. Peters, C.W., Hanlon, K.S., Ivanchenko, M.V., Zinn, E., Linarte, E.F., Li, Y., Levy, J.M., Liu, D.R., Kleinstiver, B.P., Indzhukulian, A.A., and Corey, D.P. (2023). Rescue of hearing by adenine base editing in a humanized mouse model of Usher syndrome type 1F. *Mol. Ther.* 31, 2439–2453.
  41. Jo, D.H., Jang, H.K., Cho, C.S., Han, J.H., Ryu, G., Jung, Y., Bae, S., and Kim, J.H. (2023). Visual function restoration in a mouse model of Leber congenital amaurosis via therapeutic base editing. *Mol. Ther. Nucleic Acids* 31, 16–27.
  42. Li, X., Le, Y., Zhang, Z., Nian, X., Liu, B., and Yang, X. (2023). Viral Vector-Based Gene Therapy. *Int. J. Mol. Sci.* 24, 7736.
  43. Howarth, J.L., Lee, Y.B., and Uney, J.B. (2010). Using viral vectors as gene transfer tools (Cell Biology and Toxicology Special Issue: ECTS-UK 1 day meeting on genetic manipulation of cells). *Cell Biol. Toxicol.* 26, 1–20.
  44. Lv, J., Wang, H., Cheng, X., Chen, Y., Wang, D., Zhang, L., Cao, Q., Tang, H., Hu, S., Gao, K., et al. (2024). AAV1-hOTOF gene therapy for autosomal recessive deafness 9: a single-arm trial. *Lancet.* S0140-6736:02874-X.
  45. Frangoul, H., Altshuler, D., Cappellini, M.D., Chen, Y.S., Domm, J., Eustace, B.K., Foell, J., de la Fuente, J., Grupp, S., Handgretinger, R., et al. (2021). CRISPR-Cas9 Gene Editing for Sickle Cell Disease and beta-Thalassemia. *N. Engl. J. Med.* 384, 252–260.
  46. Ledford, H. (2023). Super-precise CRISPR tool enters US clinical trials for the first time. *Nature* 621, 667–668.
  47. Wallis, B., Bowman, K.R., Lu, P., and Lim, C.S. (2023). The Challenges and Prospects of p53-Based Therapies in Ovarian Cancer. *Biomolecules* 13, 159.
  48. Hakim, C.H., Kumar, S.R.P., Pérez-López, D.O., Wasala, N.B., Zhang, D., Yue, Y., Teixeira, J., Pan, X., Zhang, K., Million, E.D., et al. (2021). Cas9-specific immune responses compromise local and systemic AAV CRISPR therapy in multiple dystrophic canine models. *Nat. Commun.* 12, 6769.
  49. Jiang, L., Wang, D., He, Y., and Shu, Y. (2023). Advances in gene therapy hold promise for treating hereditary hearing loss. *Mol. Ther.* 31, 934–950.
  50. Van der Auwera, G.A., Carneiro, M.O., Hartl, C., Poplin, R., Del Angel, G., Levy-Moonshine, A., Jordan, T., Shakir, K., Roazen, D., Thibault, J., et al. (2013). From

- FastQ data to high confidence variant calls: the Genome Analysis Toolkit best practices pipeline. *Curr. Protoc. Bioinformatics* 43, 11.10.1–11.10.33.
51. Karczewski, K.J., Francioli, L.C., Tiao, G., Cummings, B.B., Alföldi, J., Wang, Q., Collins, R.L., Laricchia, K.M., Ganna, A., Birnbaum, D.P., et al. (2020). The mutational constraint spectrum quantified from variation in 141,456 humans. *Nature* 581, 434–443.
  52. Wang, K., Li, M., and Hakonarson, H. (2010). ANNOVAR: functional annotation of genetic variants from high-throughput sequencing data. *Nucleic Acids Res.* 38, e164.
  53. Lee, J., Lee, J., Jeon, S., Lee, J., Jang, I., Yang, J.O., Park, S., Lee, B., Choi, J., Choi, B.O., et al. (2022). A database of 5305 healthy Korean individuals reveals genetic and clinical implications for an East Asian population. *Exp. Mol. Med.* 54, 1862–1871.
  54. Jung, K.S., Hong, K.W., Jo, H.Y., Choi, J., Ban, H.J., Cho, S.B., and Chung, M. (2020). KRGDDB: the large-scale variant database of 1722 Koreans based on whole genome sequencing. *Database* 2020, baaa030.
  55. Lee, S.Y., Kim, M.Y., Han, J.H., Park, S.S., Yun, Y., Jee, S.C., Han, J.J., Lee, J.H., Seok, H., and Choi, B.Y. (2023). Ramifications of POU4F3 variants associated with autosomal dominant hearing loss in various molecular aspects. *Sci. Rep.* 13, 12584.
  56. Lee, S.Y., Choi, H.B., Park, M., Choi, I.S., An, J., Kim, A., Kim, E., Kim, N., Han, J.H., Kim, M.Y., et al. (2021). Novel KCNQ4 variants in different functional domains confer genotype- and mechanism-based therapeutics in patients with nonsyndromic hearing loss. *Exp. Mol. Med.* 53, 1192–1204.
  57. Richards, S., Aziz, N., Bale, S., Bick, D., Das, S., Gastier-Foster, J., Grody, W.W., Hegde, M., Lyon, E., Spector, E., et al. (2015). Standards and guidelines for the interpretation of sequence variants: a joint consensus recommendation of the American College of Medical Genetics and Genomics and the Association for Molecular Pathology. *Genet. Med.* 17, 405–424.
  58. Schmittgen, T.D., and Livak, K.J. (2008). Analyzing real-time PCR data by the comparative C(T) method. *Nat. Protoc.* 3, 1101–1108.